2007 IEEE International Conference on
Robotics and Automation
Roma, Italy, 10-14 April 2007

μ³: Multiscale, Deterministic Micro-Nano Assembly System for Construction of On-Wafer Microrobots

Aditya N. Das, Ping Zhang, Woo H. Lee, Dan Popa, and Harry Stephanou

Abstract— **One of the major issues enduring with micro-scale mechanics has been to design high fidelity miniature machines capable of performing complex operations. Though achieved in some proportion through conventional in-plane and out-of-plane designs, the efficacy of such micro-electro-mechanical systems (MEMS) structures is highly limited due to complicate fabrication and inadequate robustness. On the other hand, the use of precise robots to assemble MEMS parts of comparatively simpler design to build 3D micromechanical structures has recently emerged as a viable approach. Such modular assemblies of microscale parts typically utilize minimum energy connectors that are multifunctional, e.g., mechanical, electrical etc. The μ^3 is a 3-D microassembly station consisting of 19 DOF arranged into 3 micromanipulators, with additional microgrippers and stereo microscope vision. The platform is capable of motion resolutions of 3nm and is small enough to be used inside of a scanning electron microscope (SEM) for nano-manipulation. In this paper we discuss how systematic identification and calibration of the station, combined with appropriate part connector designs can lead to multi-degree of freedom active MEMS robots assembled on a wafer.**

I. Introduction

The past decade has seen considerable progress made in the field of top-down precision assembly. Part of the top-down approach to accomplish micro or nano-scale assembly uses ideas from conventional assembly shrunk down in size. Examples are the use of compliant, passive MEMS microgrippers to manipulate compliant micro-parts such as in Lee et al[1], thermally actuated microgrippers using a variety of materials[4, 5], of the use of adhesive forces to manipulate microparts[2]. In addition to serial microassembly methods, others have pursued parallel manipulation techniques at small scales, for instance Bohringer et al[6] who introduced programmable force fields for manipulation with arrays of micro-actuators. Bohringer and Prasad were among the first to introduce the concept of snap-fasteners using MEMS as early as 1995[14]. A recent example of a very well designed fastener allowing 3D compliant assembly with SOI MEMS parts is the Zyvex connector[8]. Several landmark papers by Nelson, Cohn and Fearing describe and classify the architecture and algorithms used in high precision robotic cells for the purpose of directed multiscale assembly[3, 7, 8, 9]. Multiscale assembly methods can be classified based on throughput (serial or parallel), deliberate intervention (deterministic or stochastic), type of end-effectors (contact, non-contact) or level of human intervention (manual, teleoperated or automated). It has been widely accepted for some time that assembly at small scales requires not only very high precision, but also management, prediction and control of interactions from one size scale to another. Higher volume production of miniaturized devices requires the successful operation at required throughput and yield across multiple scales of tolerance, part dimension and workspace limitations.

Sequential microassembly requires a high precision micromanipulator and motion control; either by off-line programming with calibration or by on-line sensory feedback control. The later has been accomplished via a microscope or a force sensor integrated with the gripper, or both[8]. However, the price paid in assembly speed is considerable, resulting in low assembly throughputs.

With the advent of more and more diverse and intricate applications, demand for heterogeneous assemblies of micro-parts has also grown. One aim is to build entire microscale machinery (here referred as microrobots) and make it self-sustained.

In this paper we focus on deterministic serial microassembly with multiple end-effectors using the μ^3 multiscale assembly system. This system is currently in operation at our Texas Microfactory™ cleanroom. We demonstrate that high speed serial microassembly of MEMS parts can be accomplished with a high degree of reliability without servoing. Rather, the assembler follows an assembly script after a simple calibration (identification) sequence.

Manuscript received January 31, 2006. This work was supported in part by the NIST ATP Program, Office of Naval Research, and the SPRING Texas Annual Fund. The authors are with the Automation and Robotics Research Institute (ARRI), at the University of Texas at Arlington, Fort Worth, TX 76118 USA.

Aditya N. Das and Ping Zhang are pursuing doctorate studies in Electrical Engineering with Professor Popa, in the area of microrobotics.

Dan O. Popa, Ph.D. (corresponding author) is currently Assistant Professor of Electrical Engineering (e-mail: popa@arri.uta.edu). His research interests include multiscale and microrobotics, 3D microsystems integration, embedded and distributed sensors and actuators.

Woo Ho Lee, Ph.D., is currently a research faculty member with ARRI. His research interests include MEMS design and fabrication, active surface devices, and modular robotics.

Harry Stephanou, Ph.D. is Professor of Electrical Engineering and Director of ARRI. His research interests include small-scale robotics and distributed robotic systems.

1-4244-0602-1/07/$20.00 ©2007 IEEE.

The μ^3 is a 3-D microassembly station consisting of 19 DOF arranged into 3 manipulators, with additional microgrippers and stereo microscope vision. The platform is capable of motion resolutions of 3nm and is small enough to be used inside of a scanning electron microscope (SEM) for nanomanipulation. The μ^3 kinematic configuration is unique to the assembly of typical 2½D microparts fabricated on a wafer. The meso-nano μ^3 is part of a family of multiscale robotic systems being developed in our lab, including the M^3 assembly system (macro-micro)[10]. As a result, they share some of the multiscale design principles and controls.

The paper is outlined as follows; in section II we describe the μ^3, including its hardware, control and software architecture; in section III we discuss aspects related to the design and tolerance of microparts for several applications; section IV describes experimental results, including completed assemblies and calibration data; finally section V concludes the paper.

II. Description of Workcell

The μ^3 platform is a table-top 3D assembly station configured using 19 DOF discrete stages arranged into 3 robotic manipulators with 3 nm resolution. μ^3 is used to achieve both serial and deterministic parallel micro/nano scale assembly outside and inside the SEM. Figure 1 shows three μ^3 manipulators (M_1, M_2, M_3) sharing a common 25 cm^3 workspace. M_1 and M_2 are two robotic manipulator arms with 7 degrees of freedom each. They consist of XYZ coarse and fine linear stages, including the PI Nanocube® for nanoscale fine motion. A rotation stage provides a terminating roll DOF (θ) axis which is key for 3D assemblies of 2½D MEMS components. Mounted at the end of the manipulator chains are kinematic mounting pairs that provide for end-effector reconfigurability. The central manipulator M_3 is a high precision 5 DOF robot consisting of a XYθ mechanism placed on a 2 axis tilt stage. This robot carries custom designed fixtures for microparts (the dies/substrate) and a custom designed hotplate for process ability such as interconnect solder reflow.

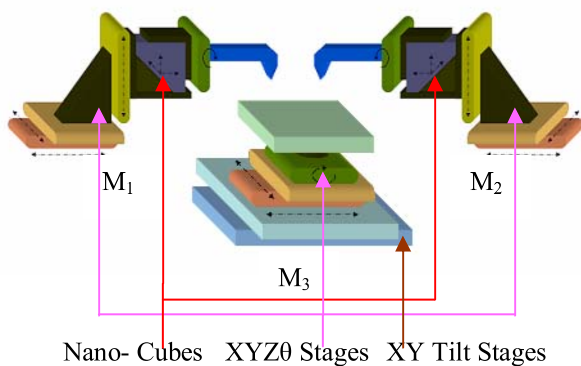

Figure 1: Schematic diagram of μ^3 (meso-micro-nano) platforms with microgrippers

A schematic diagram and picture of μ^3 is shown in Figures 1 and 2. An earlier version of a similar assembly cell was previously set up using Melles-Griot hardware[8].

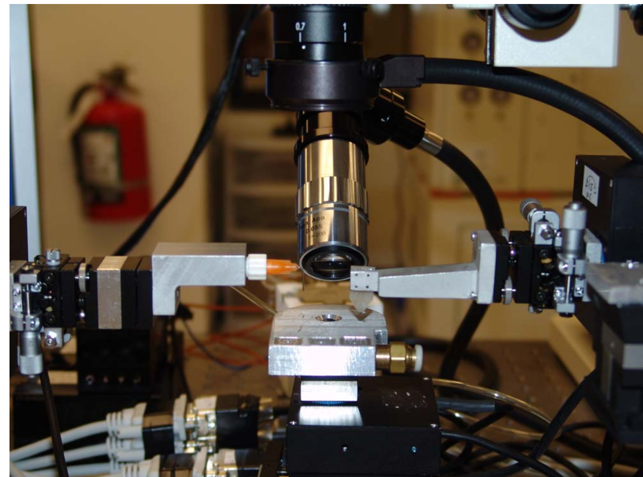

Figure 2: μ^3 assembly cell at ARRI's Microfactory

Manipulators M_1 and M_2 contain both coarse and fine positioners with a maximum motion resolution of 3nm. The total size of the workspace is approximately $8cm^3$.

To coordinate and control the operation of the multiscale robotic platforms and to automate the assembly, a set of LabVIEW® VI's have been designed and are run in supervisory mode from central PCs. These software modules provide an interactive user interface, such as the one shown in Figure 3 that provides direct user access to subsystems, algorithms and process monitors.

Figure 3: GUI for μ^3 showing video feed of a MEMS part approximately 500 µm tall gripped by a milli-nozzle

The system software manages 3D stereo vision for part location, manipulator calibration, kinematics, trajectory planning, assembly and packaging sequence execution and 1D machine vision for visual servoing during calibration. One important aspect in the kinematics of μ^3 is that XY scanning with manipulator M_3 (center) is used to "bring" the part to the end-effector, and not the other way around, how it is typically done. As a result, the end-effector will always be in focus for the 3D stereo vision system.

III. MICRO PARTS

A target application for μ³ is on-die SOI MEMS assemblies using snap-fasteners as shown in Figures 4 and 5. A microspectrometer, e.g. a die-size Si-Glass MEMS assembly accomplished using the μ³ consists of five vertical snap Si-MEMS assemblies or micromirror surfaces and lens holders, an 800μm ball lens, and a 3mm beam-splitter. Further details on the design of the MEMS parts in this application can be found in our previous work[11].

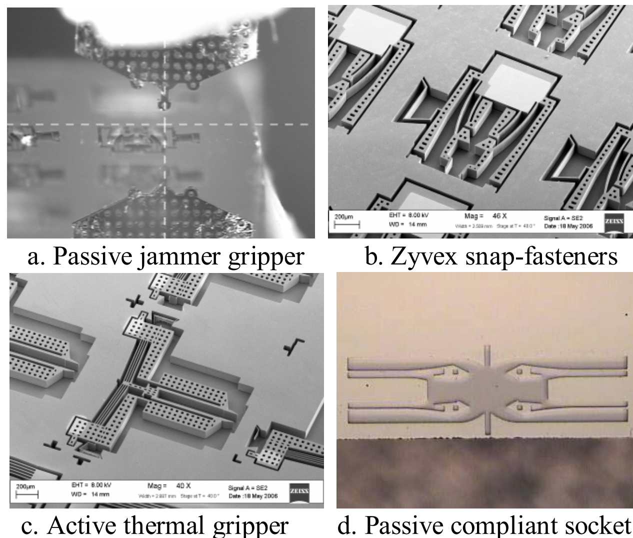

a. Passive jammer gripper b. Zyvex snap-fasteners

c. Active thermal gripper d. Passive compliant socket

Figure 4: SOI DRIE silicon micro parts for assembly

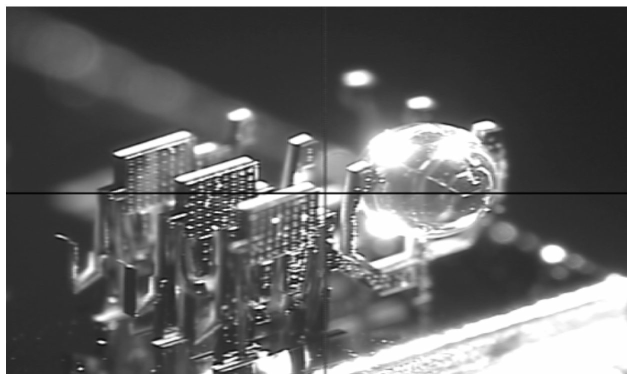

Figure 5: 3D MEMS assembly using μ³, part of a die-size microspectrometer consisting of 3 vertical DRIE silicon snap fasteners holding a 800 μm ball lens

Other types of assemblies include electrical and mechanical interconnects for active, out-of-plane multi-DOF micro scale components.

Grippers and fixtures play a very important role in assembly at multiple scales. By using precision machined fixtures, we can eliminate the need for actuator accuracies in the same range as part tolerances, and we can easily "find" the parts of interest in the assembly scene. A wafer is a fixture, so in many ways MEMS components are much easier to handle because they are already sorted. Snap-fasteners are one type of fixtures that we have already used for the assembly of silicon MEMS components. These micro-fasteners can be either active (actuated) or passive (compliant), and are used to mechanically interconnect microparts, or to fixture them to a substrate.

During microassembly, parts are passed between manipulator tools and substrate fixtures so that we observe a fundamental principle at small scales to never "let go" of the manipulated parts[8]. By using fixtures that are precision fabricated, we can automate a large part of the assembly operation by simply stepping through an "assembly script". We can thus send the slave end-effector in close proximity to the parts of interest, and we can achieve high-yield assembly operations can be accomplished without using force and vision information. Finally, in order to minimize the end-effector positioning error during assembly, the gripper tip is rotation centered, e.g. a RCR motion is achieved using vision information though a set of adjustable manual stages rotating with the θ axis of M_1 or M_3.

Snap-fit based microassembly not only compensates the positional uncertainties, but also virtually eliminates stiction problems occurring during microassembly. For the Zyvex jammers shown in Figure 4, a relative large force generated by the spring back force of the socket firmly holds the jammer into the substrate after assembly. FEA results show that the computed jammer assembly force is 18mN, and the spring back-force from the socket is 3mN which greatly exceeds the stiction force. Another advantage of using snap-fit based microassembly is that parts can be self aligned to desired location after assembly.

Tolerance analysis has popularly been used not only to predict the variations generated during assembly, but to improve the assembly capability of parts. In addition to the uncertainty of part location, the positional uncertainty of a robotic manipulator is also needed to estimate an overall uncertainty. In previous work, we showed how to characterize the assembly tolerance of MEMS components and therefore determine a "tolerance budget" for successful assembly[11,13].

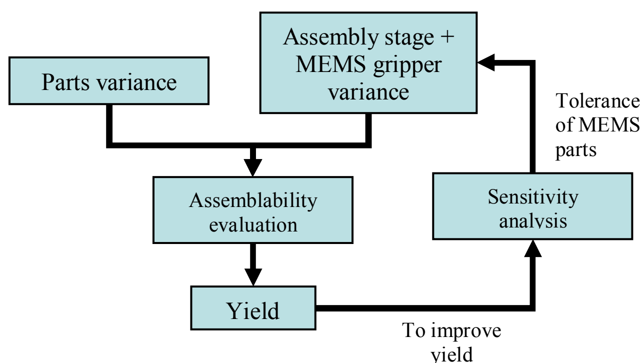

Figure 6: Iterative improvements of assembly yield using tolerance analysis.

We showed that in a certain instance of the Zyvex snap-fit, a 10μm pick tolerance and a 7μm place tolerance ensures a 3σ (±1.5σ) assembly yield distribution, if the coefficient of friction is below 1. As an aid to design compliant snap-fasteners and grippers for μ³, we have developed a tolerance analysis tool that can represent variances of parts and

assembly stages, and evaluate the assembly capability in microassembly, and the sequence of tolerance analysis is illustrated in Figure 6.

IV. CALIBRATION AND REPEATED ASSEMBLIES

Calibration (or Kinematics Identification) refers to a set of procedures for locating the robot end-effectors in a global coordinate frame. Coordination within the μ^3 system is accomplished by expressing the local coordinate frames attached to robots M_1 and M_3 in a common frame, attached to the end-effector frame of robot M_2. In a typical calibration sequence, each manipulator is commanded to several locations and the actual 3D positions are calculated using the stereo vision system. From these two sets of values (commanded position and actual position) a mapping can be derived by doing constrained least-squares fit on the data. The number of data points should be sufficient to bring the variance of the pose estimate below the robot repeatability.

Following calibration, the robots are used to perform assembly by planning operations such as MEMS snap-fastener assembly using inverse kinematics to compute the required joint coordinates that achieve necessary robot poses or visual servoing depending on part tolerance. In turn, the type of control needed for each assembly operation will ultimately determine the assembly throughput for the system and can also be optimized. Based on tolerance analysis for the Zyvex connector, 7μm calibration accuracy is sufficient for 92%+ assembly yields (within 3σ). This suggests that very high serial assembly throughput can be achieved by simply providing an "assembly script" instead of having to servo on visual information from the assembly scene.

In this paper we discuss a simple, but very effective calibration scheme based on linear interpolation of a set of taught fiducials. Consider the un-scaled coordinate frames attached to manipulator M_1 (global or encoder) and the end-effector of M_3 (die coordinates) as shown in Figure 7. Furthermore, assume that an end-effector "jammer" gripper is mounted onto M_1 and the center of this gripper is a distinct identifiable feature. For instance, it could be the gripper tip for a "rounded" jammer in Figure 4a.

At constant orientation angles relative to the substrate (typically perpendicular), the end-effector of M_1 or M_2 is used to point to reference points and its encoder joint coordinates are recorded. Using this data, the transformation of the encoder coordinate corresponding to any point in the die coordinate is calculated as:

$$R = R_1 + (R_2 - R_1)\left(\frac{p - p_1}{p_2 - p_1}\right) + (R_3 - \hat{R})\left(\frac{q - q_1}{q_3 - q_1}\right) \qquad (1)$$

$$\hat{R} = R_1 + (R_2 - R_1)\left(\frac{p_3 - p_1}{p_2 - p_1}\right)$$

If P_1, P_2 and P_3 form an orthogonal 2D coordinate system, (1) becomes simply:

$$R = R_1 + \left(\frac{p - p_1}{p_2 - p_1}\right)(R_2 - R_1) + \left(\frac{q - q_1}{q_3 - q_1}\right)(R_3 - R_1), \qquad (2)$$

Where:

- P_1, P_2, and P_3 are fiducials on the MEMS die, with die coordinates (p1, q1), (p2, q2) and (p3, q3) respectively. These values can be expressed in pixels from the CCD, or directly, in die layout coordinates, if fabrication tolerances can be neglected.
- P is an arbitrary point of interest with die coordinates (p, q). This is will later become the target assembly site.
- R_1, R_2, and R_3 are encoder vectors, corresponding to end-effector joints when the gripper tip is at locations P_1, P_2, and P_3. For a 4 DOF M1 robot, these will be 4 dimensional vectors [EncX; EncY; EncZ; Encθ].
- R is the associated M_1 joint coordinate vector when the tip is pointing to P.

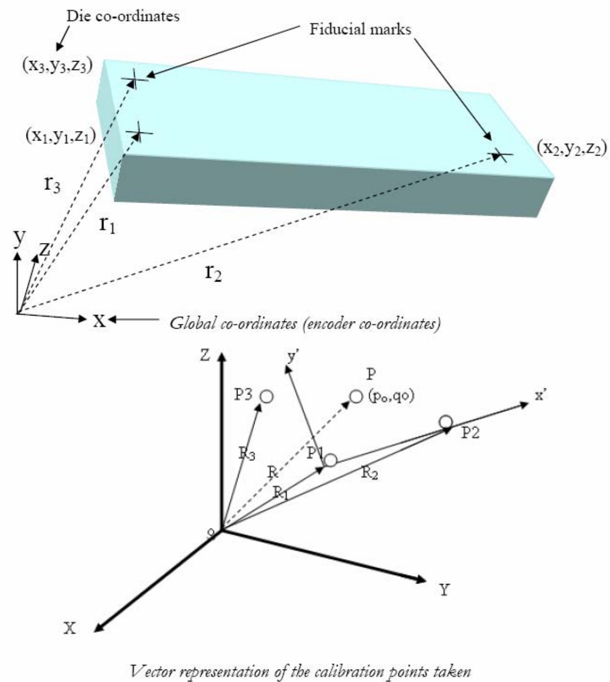

Figure 7: Rotated coordinate frames attached to M_1 and M_3 manipulators and calibration of M_1 end-effector using a 3- point teaching method.

In the following experiment, values for P_1, P_2, P_3, and P can be obtained directly from the MEMS design layout of the die, while values of R_1, R_2, and R_3 are read from the M_1 encoders. With knowledge of R, we can simply servo the joint axes of robot M_1 to position the end-effector of M_1 to pick up a part on the MEMS die at position P in die coordinates. Depending on the measurement error during the teaching phase, the inverse kinematics calculations (1) and (2) result in a given accuracy for M_1.

We have two options in estimating whether the gripper "points" to a given fiducial. In one case, the reference points are observed through a 5x objective lens that provides a 3.2 microns/pixel image resolution. As a result, a calibration error smaller than 6.4 microns (2 pixels) is expected. In the second case, we actually *physically place* the gripper tip inside a compliant feature on the die, and *visually observe* that it does not cause part shift along x, y, and z. The parts themselves are thus used for both calibration and assembly.

Figures 8 and 9 show the actual optical image and MEMS layout of the die used in our experiments.

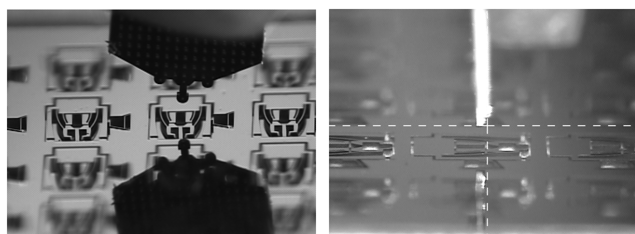

Figure 8: Microscope images from the assembly scene during calibration. A jammer end-effector is used.

The die includes an array of SOI Zyvex connectors with dimensions 800µm x 1300µm x 100µm. The microgripper is a passive "jammer" that can pick MEMS parts by means of compliant insertion.

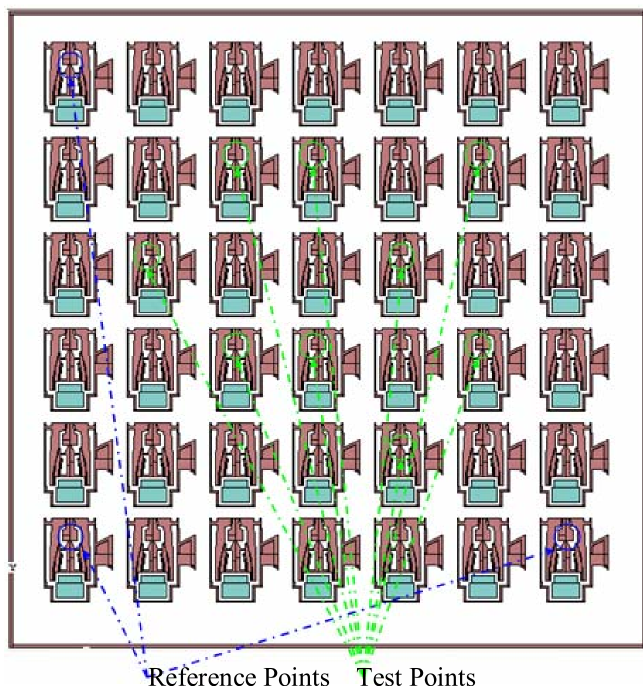

Figure 9: Layout of MEMS die, indicating 3 calibration points (left) and nine test points (right).

In this paper, we present results using 3 calibration points and 9 verification points for the layout shown in Figure 9. For the nine test points, the corresponding robot joint angles are noted by physically placing the jammer-head on these locations with visual confirmation from the stereo microscopes. Table 1 summarized the data set of the calibration experiment including a mixed joint data set, namely: x and y axes for M_3, and z joint axis for M_1. From this simple experiment we find that that the average positioning error is smaller than the 7µm value required for high assembly yield. The average positioning error is estimated to be better than 4µm on all three axes (Table 2).

Table 1: Calibration experimental data

Point	Actual Position (x, y, z) in µm	Derived Position (x, y, z) in µm	Position Error in (x, y, z) in µm	Absolute Error in (x, y, z) in µm
1	3552 7699.2 316.8	3552.78 7698.77 318.388	+0.78 +0.43 -1.588	0.78 0.43 1.588
2	4851.2 7699.2 323.2	4853.11 7700.08 319.044	-1.91 -0.88 +4.156	1.91 0.88 4.156
3	7449.6 7702.4 320	7453.64 7702.21 320.111	-4.04 +0.19 -0.111	4.04 0.19 0.111
4	2252.8 6252.8 316.8	2251.33 6248.03 318.6	+1.47 +4.77 -1.8	1.47 4.77 1.8
5	6150.4 6252.8 320	6152.13 6251.23 320.2	-1.73 +1.57 -0.2	1.73 1.57 0.2
6	3552 4697.6 316.8	3550.27 4699.17 319.8	+1.73 -1.57 -3.0	1.73 1.57 3.0
7	4851.2 4704 323.2	4850.53 4700.24 320.333	+0.67 +3.76 +2.867	0.67 3.76 2.867
8	7449.6 4697.6 323.2	7451.07 4702.37 321.4	-1.47 -4.77 +1.8	1.47 4.77 1.8
9	6150.4 3251.2 316.8	6149.56 3251.39 321.489	+0.84 -0.19 -4.689	0.84 0.19 4.689

Table 2: Mean and Standard Deviation in Error

in microns	X-Position	Y-Position	Z-Position
Mean	1.6267	2.0144	2.2457
Std Dev.	1.014	1.9067	1.5869

Note that in order to calibrate the system; we can also use an image to determine 2D vectors P_1, P_2, and P_3 instead of the direct layout location of the die sites of interest. Using the μ^3 GUI, a layout model of the assembly chip can be imported and fed into the software to identify the specific assembly. Calibration data needs to be taken in at least 3 non-collinear locations, and an inverse kinematics relationship is formed based on equation (2).

Next, a scripter implemented into the software console is used to automate the assembly process. The scripter internally compiles the assembly sequence into proper commands for the motor controllers and other supplementary peripherals and carries out the assembly process. For picking and placing of a single part, the script consists of simple commands such as:

1) Point to (pinit,qinit) on die (which translates into move M_3 in x,y to appropriate values derived from eq (2).
2) Pick up part by moving M_1 appropriately in z.
3) Rotate part 90 degrees using M_1
4) Point to (pfinal, qfinal) with picked up part. Here a small correction needs to be made to account for the fact that we are pointing not with the gripper tip, but with a micropart that is picked up by the gripper.

5) Place part by moving appropriately in z.
6) Repeat to next part.

In the future, advanced features such as path planning, collision avoidance to strengthen the assembly throughput and yield on the μ³. Figures 10 and 11 show images of repeated MEMS assemblies obtained using this method. Some of the SEM photographs contain active sockets and active out of plane actuators (such as a vertically assembled gripper). The active components are actuated through wire-bonds and reflown solder connectors that increase the mechanical stiffness of the snap-fastener. These basic building blocks will be utilized in the future to construct 3+ DOF MEMS robots that are entirely located on substrate.

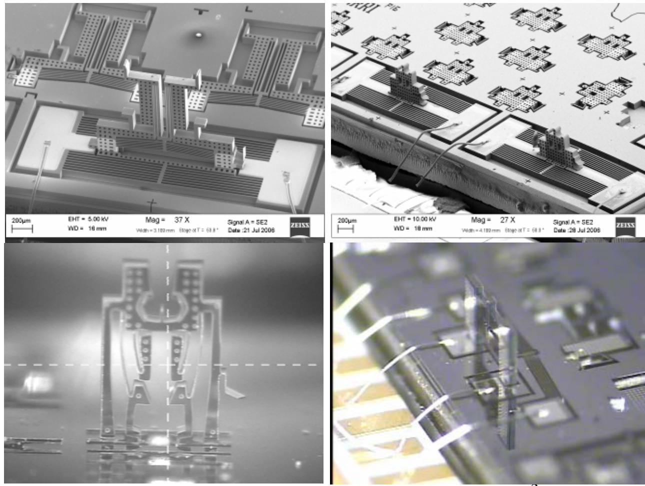

Figure 10: Examples of micro assemblies using μ^3, including 50 μm thick SOI thermal MEMS with out of plane passive and actuated grippers, as well as active (0-force sockets).

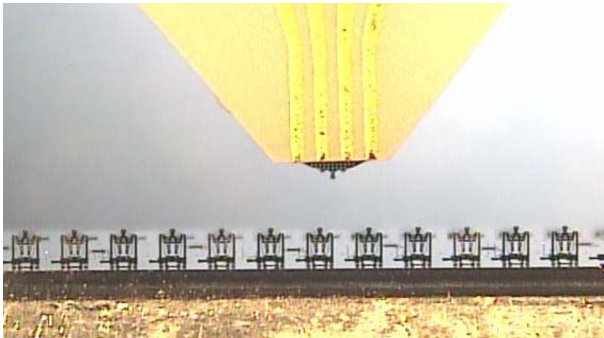

Figure 11: A row of standing passive Zyvex jammers obtained by calibration and assembly scripting. Assembly yield was 100% (12 out of 12) in this case.

V. Conclusion and Future Works

In this paper we present a systematic approach to address precision and throughput issues in MEMS assembly. With experimental results and successful assemblies we conclude that advanced system identification, calibration techniques and proper selection and designing of microparts can implement the assembly comparatively simpler and faster. Future work involves study of stochastic parallel micro assembly, exponential or self assembly of micro parts to increase the assembly throughput, nano scale assemblies, and assembly of multi-DOF active MEMS robots.

References

[1] W.H. Lee, B.H. Kang, et. al., "Micropeg manipulation with a compliant microgripper", *in Proceedings of IEEE International Conference on Robotics and Automation*, Washington, D.C., 2002.

[2] F. Arai, T. Fukuda, "Adhesion-type micron-endeffector for micromanipulation," *in Proceedings of IEEE International Conference on Robotics and Automation*, pp.1472-1477, 1997.

[3] Y. Zhou, B.J. Nelson, and B. Vikramaditya, "Fusing force and vision feedback for micromanipulation," *in Proceedings Of IEEE International Conference on Robotics and Automation*, Leuven, Belgium, May 1998.

[4] G. Greitmann and R. A. Buser, "Tactile microgripper for automated handling of microparts," *Sensors and Actuators*, A.53, pp.410- 415, 1996.

[5] M. Shimada, J. A. Tompson, J. Yan, R. J. Wood, and R. S. Fearing, "Prototyping millirobots using dextrous microassembly and folding," *in Proceedings of ASME IMECE/DSCD*, vol.69-2, pp.933-940, 2000.

[6] K. F. Bohringer, et. al., "Sensorless manipulation using massively parallel microfabricated actuator arrays," *in Proceedings of IEEE International Conference on Robotics and Automation*, pp.826-833, 1998.

[7] K. Goldberg, K.F. Bohringer, R. Fearing, "Microassembly," *in Handbook of Industrial Robotics, 2nd Edition, edited by S. Nof. John Wiley and Sons*, 1999, pp 1045-1066.

[8] D.O.Popa, H.Stephanou, "Micro and meso scale robotic assembly", *in SME Journal of Manufacturing Processes*, Vol. 6, No.1, 2004, 52-71.

[9] A.A. Rizzi, J. Gowdy, R.L. Hollis, "Agile assembly architecture: an agent based approach to modular precision assembly systems," *in Proceedings of IEEE International Conference on Robotics and Automation*, Volume: 2, 20-25 April 1997, pp 1511 – 1516.

[10] D.O. Popa, R. Murthy, et al., "M3-Modular multi-scale assembly system for MEMS packaging", *in Proceedings of IEEE/RSJ International Conference on Intelligent Robots and Systems (IROS '06)*, Beijing, China, October 2006.

[11] W. H. Lee, D.O. Popa, et.al., "Compliant microassembly of MEMS," *in Proceedings of ANS Conference for Emergencies and Hazardous Environments*, Salt Lake City, Utah, February 2006.

[12] N. Dechev, W.L. Cleghorn, and J.K. Mills, "Microassembly of 3-D microstructures using a compliant passive micro gripper," *Journal of MEMS*, Vol. 13, No. 2, April 2004.

[13] W. H. Lee, M. Dafflon, H.E. Stephanou, Y.S. Oh, J. Hochberg, and G. D. Skidmore, "Tolerance analysis of placement distributions in tethered micro-electro-mechanical systems components," *in Proceedings of IEEE International Conference on Robotics and Automation*, May, 2004.

[14] R. Prasad, K.-F. Bohringer, N.C. MacDonald, "Design, Fabrication, and Characterization of Single Crystal Silicon Latching Snap Fastners for Micro Assembly," *in Proceedings of ASME International Mechanical Engineering Congress and Exposition (IMECE '95)*, San Francisco, CA, Nov. 1995.